Design Considerations for the Beam-Waveguide Retrofit of a Ground Antenna Station

T. Veruttipong, J. Withington, V. Galindo-Israel,
W. Imbriale, and D. Bathker
Radio Frequency and Microwave Subsystems Section

Retrofitting an antenna that was originally designed without a beam waveguide introduces special difficulties because it is desirable to minimize alteration of the original mechanical truss work and to image the actual feed without distortion at the focal point of the dual-shaped reflector. To obtain an acceptable image, certain Geometrical Optics (GO) design criteria are followed as closely as possible. The problems associated with applying these design criteria to a 34-meter dual-shaped DSN antenna are discussed. The use of various diffraction analysis techniques in the design process is also discussed. GTD and FFT algorithms are particularly necessary at the higher frequencies, while Physical Optics and Spherical Wave Expansions proved necessary at the lower frequencies.

I. Introduction

A primary requirement of the NASA Deep Space Network (DSN) is to provide for optimal reception of very low signal levels. This requirement necessitates optimizing the antenna gain to the total system operating noise level quotient. Low overall system noise levels of 16 to 20 K are achieved by using cryogenically cooled preamplifiers closely coupled with an appropriately balanced antenna gain/spillover design. Additionally, high-power transmitters (up to 400 kW CW) are required for spacecraft emergency command and planetary radar experiments. The frequency bands allocated for deep space telemetry are narrow bands near 2.1 and 2.3 GHz (S-band), 7.1 and 8.4 GHz (X-band), and 32 and 34.5 GHz (Ka-band). In addition, planned operations for the Search for Extraterrestrial Intelligence (SETI) program require continuous low-noise receive coverage over the 1 to 10 GHz band. To summarize, DSN antennas must operate efficiently with low receive noise and high-power uplink over the 1 to 35 GHz band.

Feeding a large low-noise, ground-based antenna via a beam-waveguide system has several advantages over directly placing the feed at the focal point of a dual-shaped antenna. For example, significant simplifications are possible in the design of high-power, water-cooled transmitters and low-noise cryogenic amplifiers, since these systems do not have to rotate as in a normally fed dual reflector. Furthermore, these systems and other components can be placed in a more accessible location, leading to improved service and availability. Also, the losses associated with rain on the feedhorn radome

are eliminated because the feedhorn can be sheltered from weather.

Many existing beam-waveguide systems use a quasi-optical design, based on Guassian wave principles, which optimizes performance over an intended operating frequency range. These designs can be made to work well with relatively small reflectors (a very few tens of wavelengths), and may be viewed as "bandpass," since performance suffers as the wavelength becomes very short as well as very long. The long wavelength end is naturally limited by the approaching small D/λ of the individual beam reflectors used; the short wavelength end does not produce the proper focusing needed to image the feed at the dual-reflector focus. In contrast, a purely geometrical optics (G.O.) design has no upper frequency limit, but performance suffers at long wavelengths. These designs may be viewed as " high pass." Considering the need for practically sized beam reflectors and the high DSN frequency and performance requirements, the G.O. design is favored in this application.

Retrofitting an antenna that was originally designed without a beam waveguide introduces special difficulties because it is desirable to minimize alteration of the original structure. This may preclude accessing the center region of the reflector (typically used in conventional beam-waveguide designs), and may require bypassing the center region. A discussion of the mechanical tradeoffs and constraints is given herein, along with a performance analysis of some typical designs. In the retrofit design, it is also desirable to image the original feed without distortion at the focal point of the dual-shaped reflector. This will minimize gain loss, reflector design, and feed changes.

To obtain an acceptable image, certain design criteria are followed as closely as possible. In 1973, Mizusawa and Kitsuregawa (Ref. 1) introduced certain G.O. criteria which guarantee a perfect image from a reflector pair (cell). If more than one cell is used (where each cell may or may not satisfy Mizusawa's criteria), application of other G.O. symmetry conditions can also guarantee a perfect image. The problems and opportunities associated with applying these conditions to a 34-m dual-shaped antenna are discussed.

The use of various diffraction analysis techniques in the design process is also discussed. Gaussian (Goubau) modes provide important insight to the wave propagation characteristics, but Geometrical Theory of Diffraction (GTD), FFT, Spherical Wave Expansion (SWE), and Physical Optics (PO) have proven more accurate and faster. The GTD and FFT algorithms are particularly necessary at the higher frequencies. Both PO and SWE have been necessary at the lower frequencies.

II. Design Considerations

A. High-Pass Design Feed Imaging

For a 2.4-m (8-foot) reflector beam waveguide operated over 1 to 35 GHz with near perfect imaging at X-band and Ka-band and acceptable performance degradation at L-band (1.68 GHz) and S-band, a high-pass type beam waveguide should be used. This type of design is based upon G. O. and Mizusawa's criteria. Mizusawa's criteria can be briefly stated as follows:

For a circularly symmetric input beam, the conditions on a conic reflector pair necessary to produce an identical output beam are:

(1) The four loci (two of which may be coincident) associated with the two curved reflectors must be arranged on a straight line.

(2) The eccentricity of the second reflector must be equal to the eccentricity or the reciprocal of the eccentricity of the first reflector.

Figure 1 shows some of the orientations of the curved reflector pair that satisfy Mizusawa's criteria. We term a curved reflector pair as one cell.

For the case of two cells where at least one cell does not satisfy Mizusawa's criteria, a perfect image may still be achieved by imposing some additional conditions, described below.

Let S_1, S_2, S_3, and S_4 be curved surfaces of two cells as shown in Fig. 2. Each surface can be an ellipsoid, hyperboloid, or paraboloid. Keeping the same sequence order, the surfaces are divided into two pairs [first pair (S_2, S_3); second pair (S_1, S_4)] as shown in Fig. 2.

For a circularly symmetric input pattern, an identical output pattern (in the G.O. limit) can be obtained if Mizusawa's criteria are satisfied for both pairs in the following manner: First pair (S_2, S_3) satisfies Mizusawa's criteria; second pair (S_1, S_4) satisfies Mizusawa's criteria after eliminating the first pair.

It is noted that the first pair can be eliminated because the input is identical to the output. Also, this concept can be applied to cases with more than two cells. Examples of an extension of Mizusawa's criteria for a multiple-reflector beam waveguide are given in Figs. 3 and 4.

Figure 5 shows a geometrical optics field reflected from each reflector of a beam-waveguide system. (Refer to Fig. 3 [a] .) It is clear from Fig. 5 that the distorted pattern from the first

cell is completely compensated for by the second cell and yields an output pattern identical to the input pattern.

B. Bandpass Design Feed Imaging

For many systems, a single-frequency or bandpass design can be advantageously employed. The design considerations can best be described with reference to Fig. 6, where the center frequency is given as f_0, and L_2 is the spacing between two curved surfaces. A bandpass beam-waveguide system is usually composed of two non-confocal (shallow) ellipsoids (eccentricity close to one). Again from Fig. 6, F_{A1} and F_{A2} are G.O. foci of ellipsoid A, while F_{AP} is the phase center of the scattered field from surface A (evaluated at frequency = f_0) in the neighborhood of surface B. Similarly, F_{B1}, F_{B2}, and F_{BP} are for ellipsoid B. The distances from F_{A2} and F_{AP} to surface A are very large compared to L_1 and L_2. The locations of F_{AP} and F_{BP} depend on frequency as well as surface curvature, L_1, and L_2. For example, with a 2.4-m reflector with eccentricity = 0.97 at f = 2.3 GHz and L_2 = 8 m (26 feet), F_{AP} is about 120 m (400 feet) to the *left* of ellipsoid A, as shown in Fig. 6(a). In the G.O. limit, F_{AP} and F_{A2} are at the same location, to the *right* of ellipsoid A.

It is desirable to have two identical surfaces for low cross-polarization and a symmetrical system. Trial and error are needed in order to determine surface parameters for the desired operating frequency and bandwidth within specified losses.

Figure 7 shows the input and output patterns from a bandpass beam-waveguide system where F_{AP} and F_{BP} are chosen to be at the same locations as F_{B2} and F_{A2}, respectively (the choice may not be the optimum condition). The two identical ellipsoids are designed at f_0 = 2.3 GHz. The results show good agreement between the input feed and the imaged feed. Bandpass beam-waveguide systems appear useful when a limited band coverage is required, using modestly sized (D = 20 to 30λ) reflectors. However, these systems do not perform well as the wavelength approaches either zero or infinity. In contrast, a high-pass (G.O.) design focuses perfectly at zero wavelength and focuses very well down to $D \sim 40\lambda$. The performance then decreases monotonically as D becomes smaller in wavelength.

III. Application Considerations for the DSN

The DSN presently operates three 34-m high efficiency (H.E.) dual-shaped reflector antennas with a dual-band (2.3/8.4-GHz) feed having a far-field gain of +22.4 dBi that is conventionally located at the Cassegrain focal point. The structures were designed prior to the beam-waveguide requirements, and feature a continuous elevation axle and a carefully designed elevation wheel substructure. The elevation wheel substructure, shown in Fig. 8, plays a key role in preserving main reflector contour integrity as the antenna rotates in elevation. To maintain contour integrity at 8 GHz and above is of prime concern for RF efficiency performance as well as retrofit costs. Figure 9 shows a centerline beam-waveguide approach which, although it is a compact and straightforward RF design, severely impacts retrofit costs and the contour integrity of the main reflector (hence RF efficiency at 8 GHz and above). Figure 10 shows an unconventional approach and represents attempts to reduce structural impacts. Figure 10 is a six-reflector beam waveguide (eight-reflector antenna) based on our extension of Mizusawa's criteria. Although several detailed options are possible, most options use two cells (four curved reflectors) with two flat reflectors. Some of the options make use of the flexibility afforded by allowing each cell to be distorting (of itself), but then compensated for by the second cell as described in Figs. 3, 4, and 5.

The goal is therefore to perfectly image a feed located perhaps 15 to 25 m (50 to 80 feet) below the main reflector to the original Cassegrain focus. This goal applies over the 1 to 35-GHz frequency range, using a beam-waveguide housing limited to about 2.4 m (8 feet) in diameter. The image should be a 1:1 beamwidth transformation of the original +22.4 dBi feed, permitting reuse of that feed and no changes to the subreflector or main reflector contour. Lastly, the goal includes minimal structural impacts, particularly to the integrity of the main reflector contour. The generalized solution to these goals is reflected in the approach shown in Fig. 10, termed the bypass beam waveguide.

IV. Analytical Techniques for Design and Analysis

The software requirements for the study and design of beam waveguides are extensive. These include the capability for G.O. synthesis, Gaussian wave analysis, and high and low frequency diffraction analysis. These requirements are discussed below.

A. Geometrical Optics Synthesis Capability

This capability includes software which synthesizes as well as analyzes reflectors satisfying the Mizusawa-Kitsuregawa conditions (Ref. 1) for minimum cross-polarization and best imaging.

In the high-frequency domain (8 to 35 GHz for the designs considered herein), the focused system shown in Fig. 11 is desired. Of course, two paraboloids or mixtures of various conic-section reflectors can be synthesized. Optimization at

lower frequency bands generally is accomplished by appropriate defocusing.

B. Gaussian Wave Analysis Capability

The required defocusing for the lower bands can be determined by using various beam imaging techniques (Ref. 2) which are based on Gaussian beam analysis methods first developed by Goubau and Schwering (Ref. 3). While Gaussian mode analysis is useful at high as well as low frequencies for "conceptual" designing, conventional diffraction analysis methods are found to be more suitable.

One consideration is that Gaussian mode analysis does not supply spillover losses directly with as great an accuracy as conventional diffraction analysis methods. The Gaussian modes supply the discrete spectrum, whereas the spillover losses are directly related to the continuous spectrum (Ref. 4, pp. 474–475). Spillover for Gaussian modes is computed by a method more suitable in terms of computational efficiency for a great number of reflection (refraction) elements (Ref. 3). The antenna systems considered here rarely contain more than four curved reflectors. Further, spillover losses must be reliably known to much less than a tenth of a decibel for high performance systems.

C. Low Frequency Diffraction Analysis Capability

Because of the large bandwidth of operation (1 to 35 GHz), there is no single diffraction analysis method which will be both accurate and efficient over the entire band.

Efficiency, in the sense of speed of computation, is critical, since in a constrained design many different configurations may be analyzed before an optimum beam-waveguide configuration is selected.

In the region of 2.3 GHz (for the 34-m antenna considered herein), the reflector diameters are generally about 20λ. Since a very low edge taper illumination, at least −20 dB, is used to reduce spillover loss, the "effective" reflector diameters are very small in this frequency range.

A comparison between three diffraction algorithms: PO, GTD, and Jacobi-Bessel (JB) leads to the conclusion that:

(1) GTD is not sufficiently accurate at the low frequencies.

(2) JB is very slowly convergent in many cases and gives only the far-field in any case. We must determine near-field patterns.

(3) PO is both accurate and sufficiently fast below 3 GHz.

The above results are illustrated in Figs. 12 and 13 when an actual +22.4 dBi corrugated feedhorn is used. It can be seen from Fig. 13 that PO and JB agree perfectly to ~±20 deg.

There are two general PO computer algorithms useful at the low frequencies. One is a straightforward PO algorithm which subdivides the reflectors into small triangular facets. This is essentially a trapezoidal integration of the near-field radiation integral and is a very flexible algorithm.

A second algorithm is based on a Spherical Wave Expansion (SWE) and is also a PO technique. It has two useful characteristics: (1) when a high degree of circular symmetry exists in the scattered fields, then the two-dimensional radiation integral is reduced to a small number of one-dimensional integrals with a resultant marked decrease of computational speed; and (2) an r interpolation of the scattered field (at different radial distances from the coordinate origin) is done very accurately.

The PO (direct-trapezoid) and SWE algorithms are useful for cross-checking results. Near-field and far-field computations and comparisons in both amplitude and phase are shown in Figs. 14, 15, and 16. Figure 14 contains near-field PO and SWE results for scattering from one paraboloid reflector. Figure 15 contains the results for far-field scattering from two reflectors. Figure 16 contains the near-field scattering for two reflectors and a comparison of the "imaging" with the feed pattern. At higher frequencies (>8 GHz), the feed pattern will be virtually perfectly imaged over an angle of ±15 deg.

D. High Frequency Diffraction Analysis Capability

For reflector diameters of 70 or more wavelengths (>8 GHz), including a −20 dB edge taper, PO analysis methods become too expensive and time consuming. (The SWE may still be useful if a high degree of rotational symmetry exists.) An alternative approach is to use GTD analysis. The GTD computation speed does not increase with increasing reflector diameters, but the accuracy of the analysis does increase.

In order to test the accuracy of GTD at 8 GHz, comparisons were made between GTD and PO. Results for diffraction of a single ellipsoid are shown in Fig. 17. The results for the phase of the scattered field were equally as good. GTD was determined to be accurate at 8 GHz and higher.

Analysis of two or more reflectors by GTD involves some manipulation of the fields scattered between any two reflectors. The fields scattered from one reflector must be placed in a format suitable for GTD scattering from the next reflector. This is accomplished by computing the vector-scattered field in the vicinity of the next reflector and then interpolating as follows:

(1) Use of an FFT for ϕ-variable interpolation.

(2) Use of a second-order Lagrangian local interpolation for θ interpolation (for a z-axis along the axis of the reflector, ϕ and θ are spherical coordinates).

(3) For the r (of $[r, \theta, \phi]$ spherical coordinates) interpolation, an approximation consistent with the GTD approximation was to assume a $1/r$ variation in amplitude and a kr variation in phase. This approximate interpolation should be checked against exact computations of the near fields.

By the method described above, multiple reflector computations, even with a large number of reflectors, can be calculated with both great speed and accuracy at frequencies above ~8 GHz for reflectors of $>70\lambda$ in diameter.

A typical result is shown in Fig. 18 for a pair of ellipsoids which satisfy the Mizusawa-Kitsuregawa criteria. The object is to perfectly image the input feed over about ±20 deg. This is accomplished with great accuracy and virtually no loss at X-band frequencies and higher.

V. Conclusions

A generalized solution has been achieved for retrofitting a large dual-shaped reflector antenna for beam waveguide. The design is termed bypass beam waveguide. Several detailed options within the bypass category remain to be studied, and work continues.

With the analysis capability available, we are gaining some valuable views of the RF performance behavior of some of the many options. It appears fairly clear for the 1 to 35-GHz requirement that high-pass (pure G.O.) designs are necessary in contrast to a bandpass (non-confocal ellipsoids) approach. It appears that deep confocal ellipsoids satisfying the Mizusawa-Kitsuregawa criteria operate (focus) well with reflector diameters of about 70 and larger but may not be tolerable at longer wavelengths.

As a part of this activity, an important extension of the Mizusawa-Kitsuregawa criteria has been revealed. The principle revealed shows how a two-reflector cell, although in itself distorting, may be combined with a second cell which compensates for the first and delivers an output beam which is a good image of the input beam.

References

1. Mizusawa, M., and Kitsuregawa, T., A Beam Waveguide Feed Having a Symmetric Beam for Cassegrain Antennas, *IEEE Trans. Antennas and Propagat.*, pp. 844–886, November 1973.
2. Chu, T. S., An Imaging Beam Waveguide Feed, *IEEE Trans. Antennas and Propagat.*, pp. 614–619, July 1983.
3. Goubau, G., and Schwering, F., On the Guided Propagation of Electromagnetic Wave Beams, *IRE Trans. Antennas and Propagat.*, pp. 248–256, May 1961.
4. Collin, R. E., *Field Theory of Guided Waves*, McGraw-Hill, N.Y., 1960.

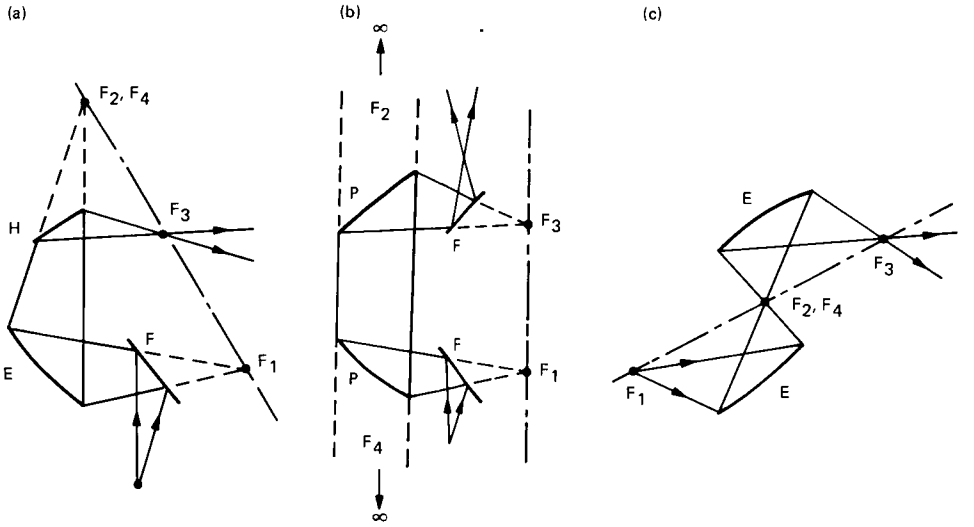

Fig. 1. Possible two-curved reflector beam-waveguide configurations; E = ellipsoid, H = hyperboloid, P = paraboloid, F = flat plate

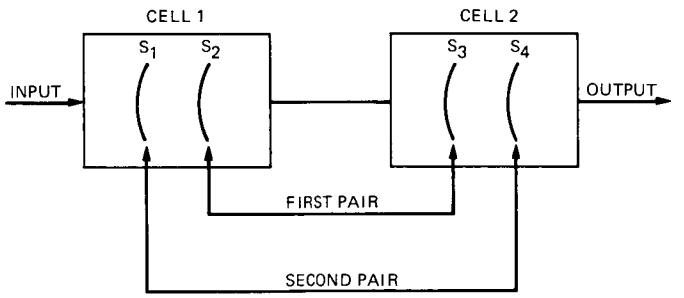

Fig. 2. Multiple curved reflector beam-waveguide system; S_1 = ellipsoid, hyperboloid, or paraboloid

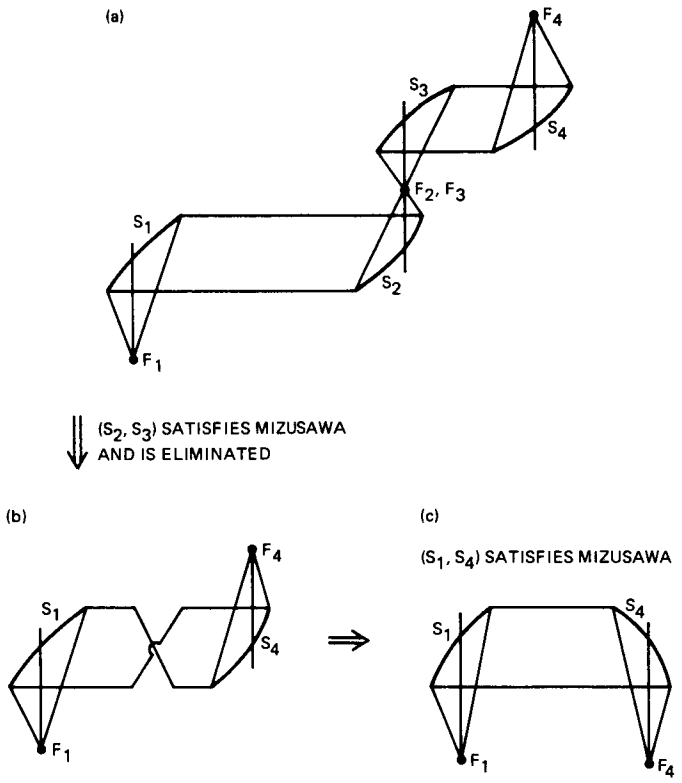

Fig. 3. Demonstrating an extension of Mizusawa's criteria for a multiple reflector beam waveguide (paraboloids)

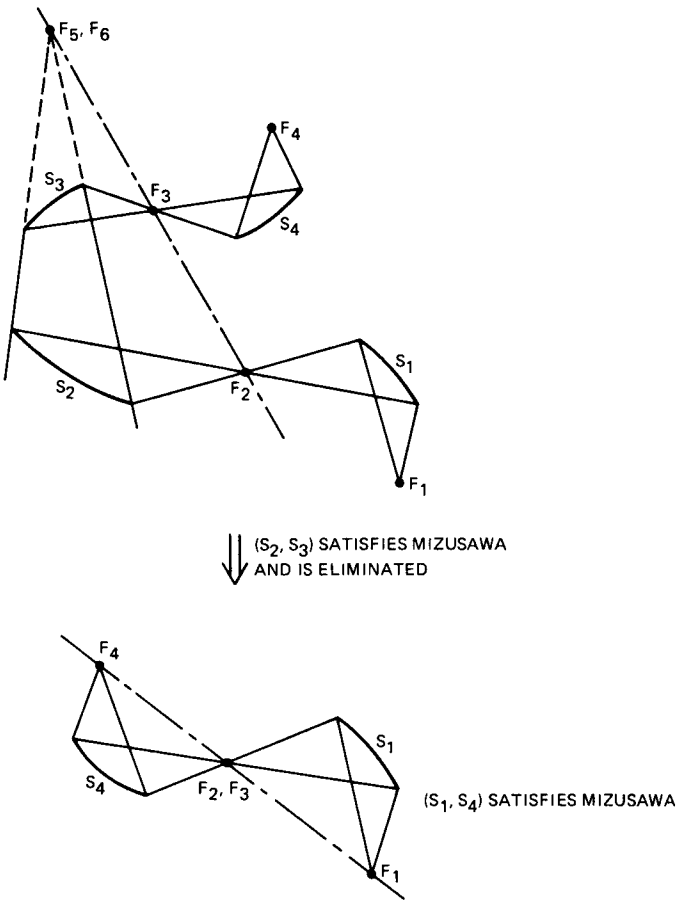

Fig. 4. Demonstrating an extension of Mizusawa's criteria for a multiple reflector beam waveguide (ellipsoids/hyperboloids)

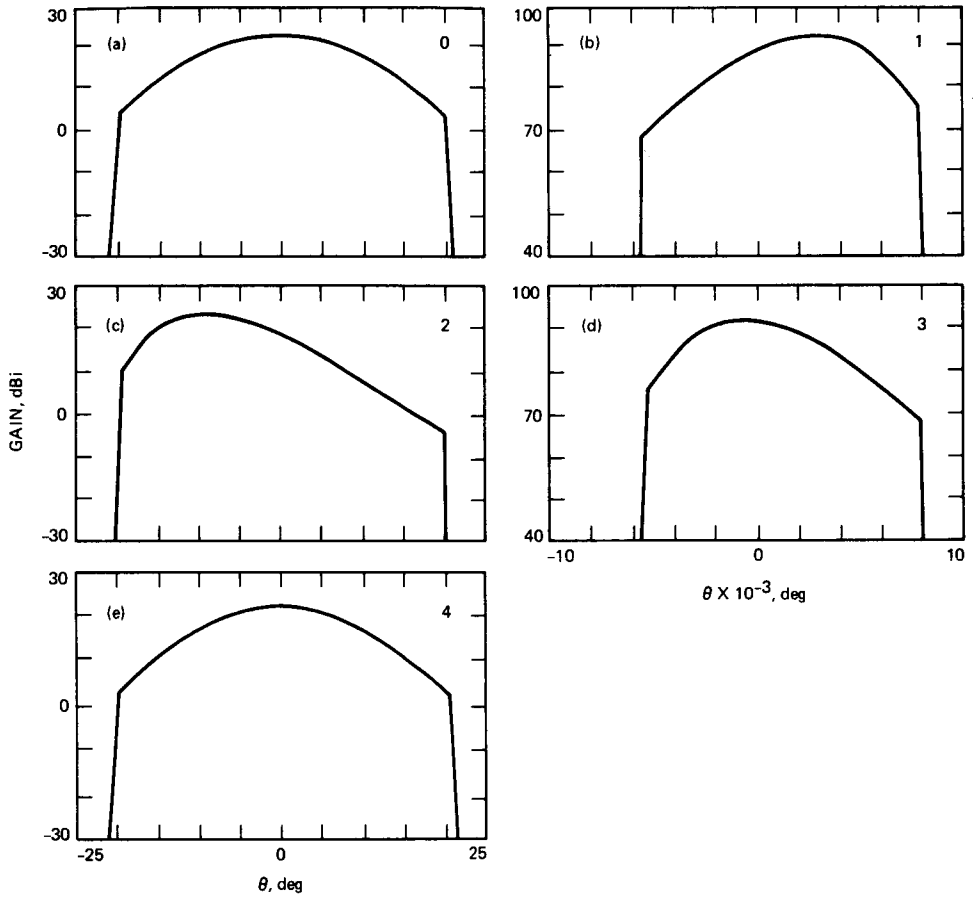

Fig. 5. Geometrical optics field reflected from each surface of a beam-waveguide system (shown in Fig. 3[a]): (a) input pattern; (b) reflected field from S_1; (c) reflected field from S_2; (d) reflected field from S_3; (e) reflected field from S_4 or output pattern

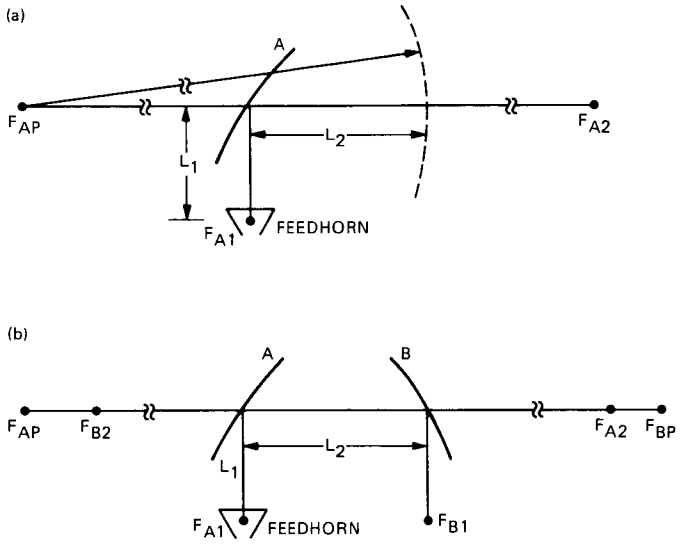

Fig. 6. Bandpass feed imaging configuration

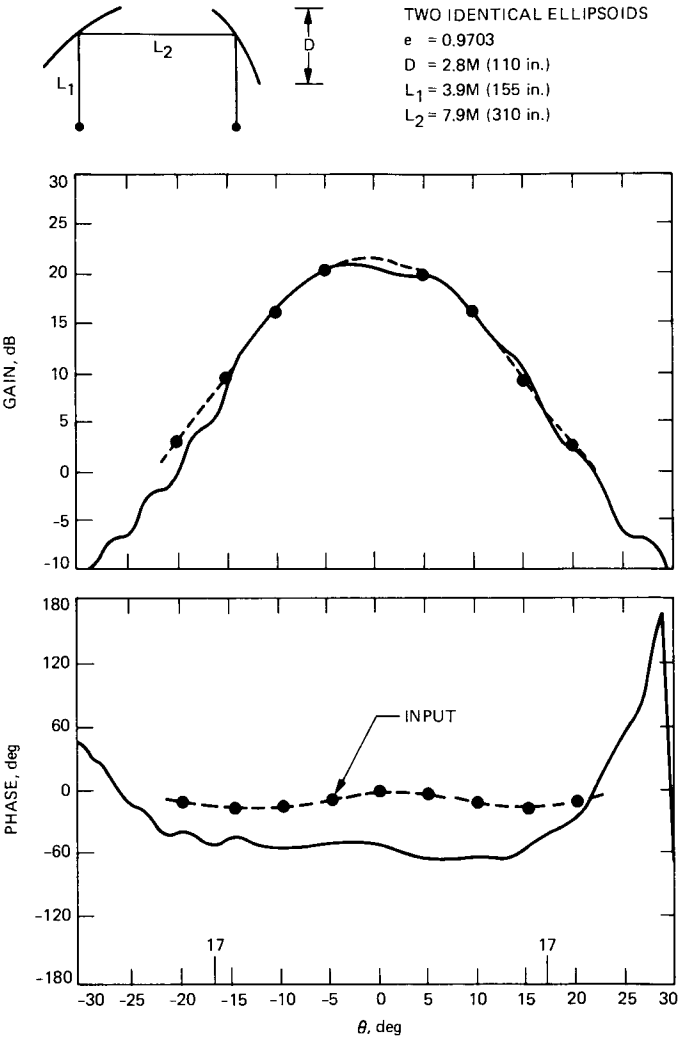

Fig. 7. Comparison between input feed pattern and feed image from a bandpass beam-waveguide system at center frequency = 2.3 GHz

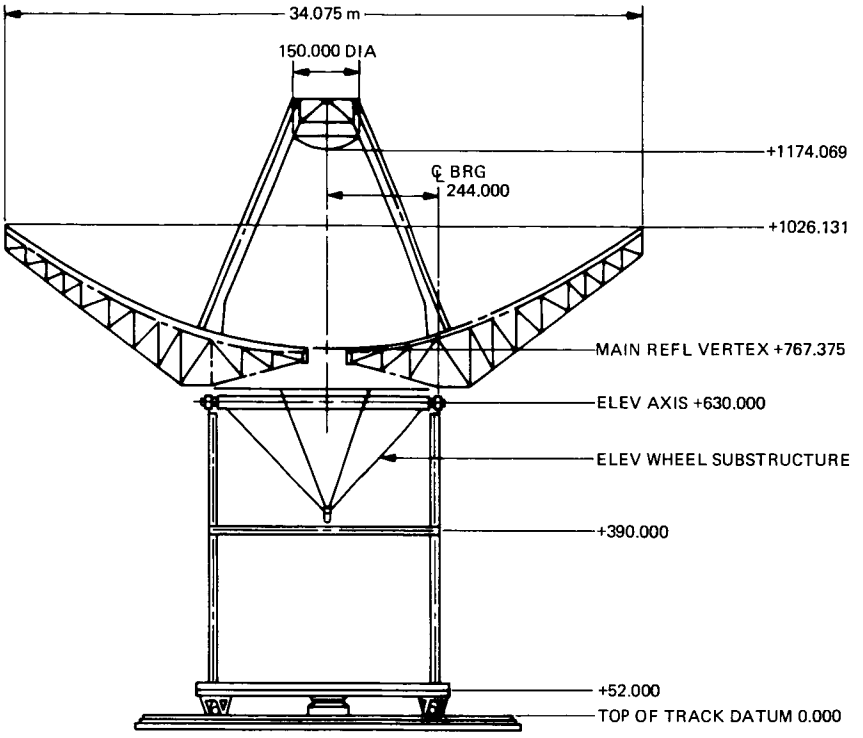

Fig. 8. 34-m H.E. existing structure

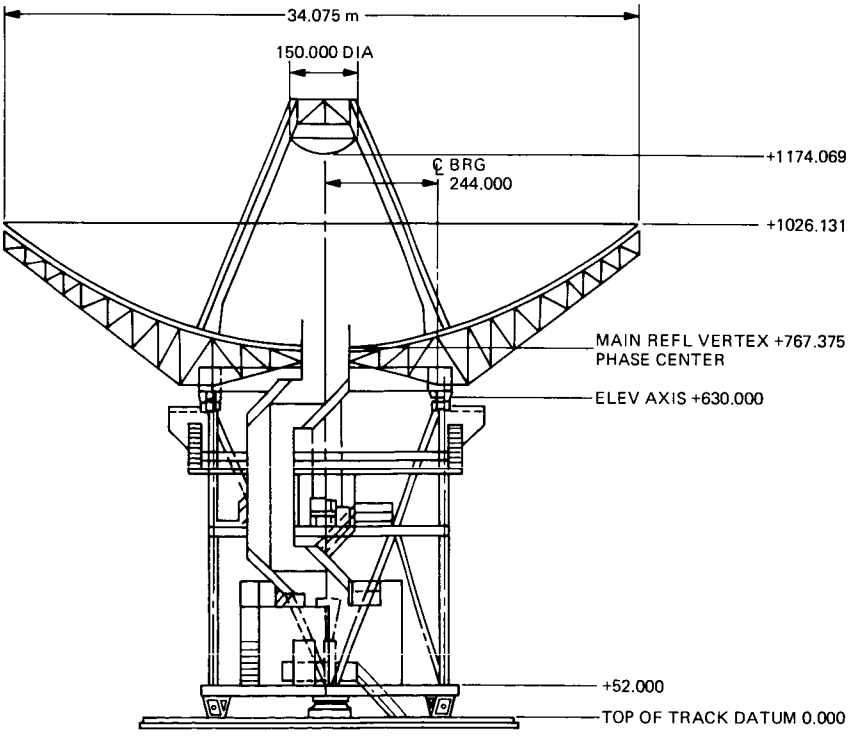

Fig. 9. 34-m H.E. centerline beam waveguide

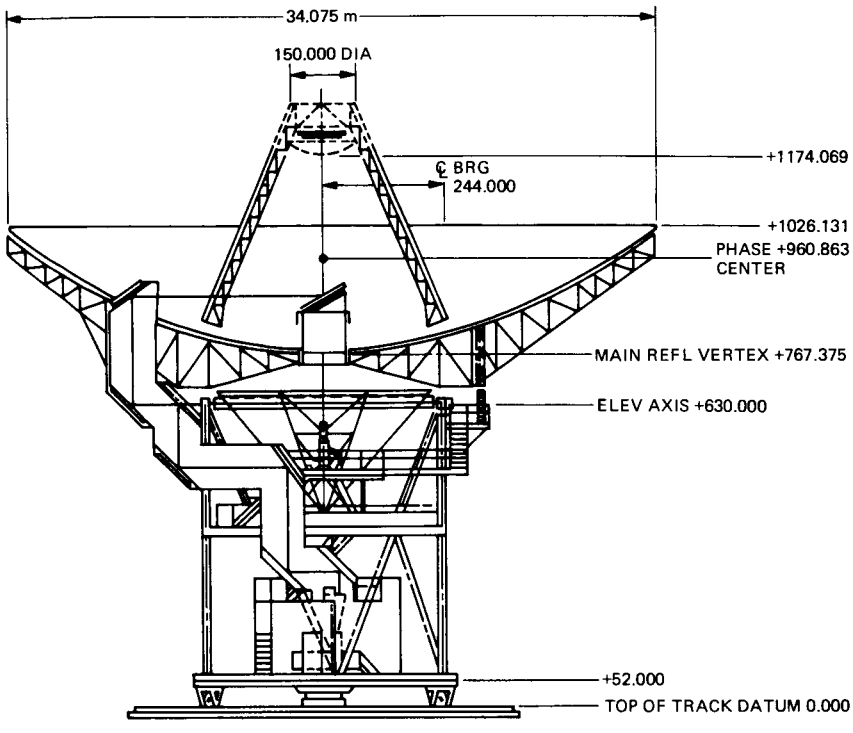

Fig. 10. 34-m H.E. bypass beam waveguide

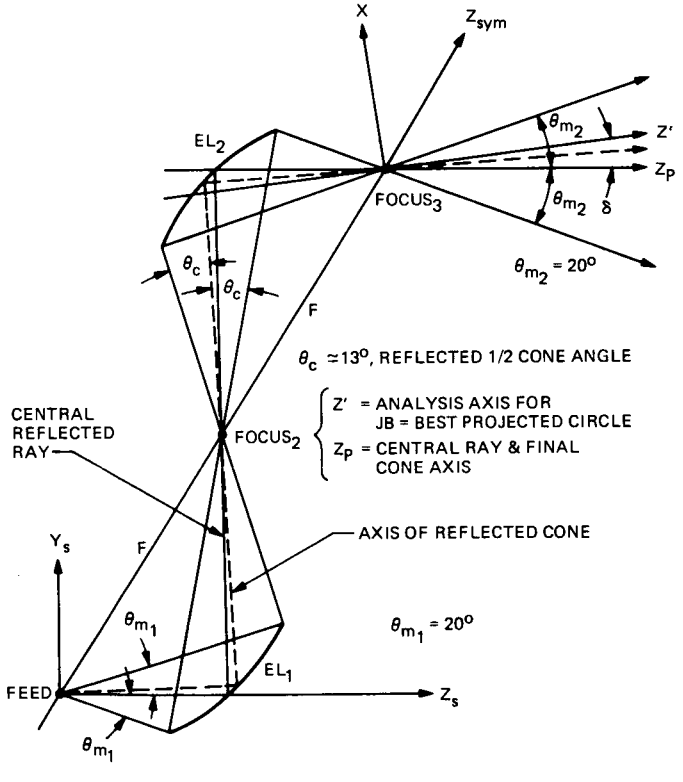

Fig. 11. Analysis geometry for ellipsoid pair (EL_1, EL_2)

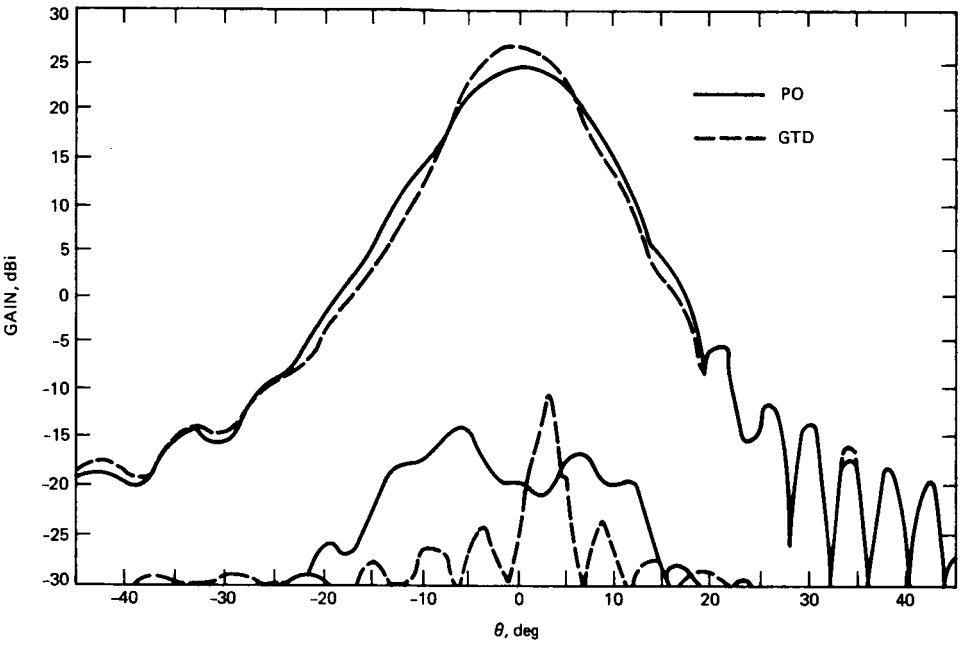

Fig. 12. Near-field, one 2.4-m ellipse diffraction patterns (RCP, 2.3-GHz, offset plane)

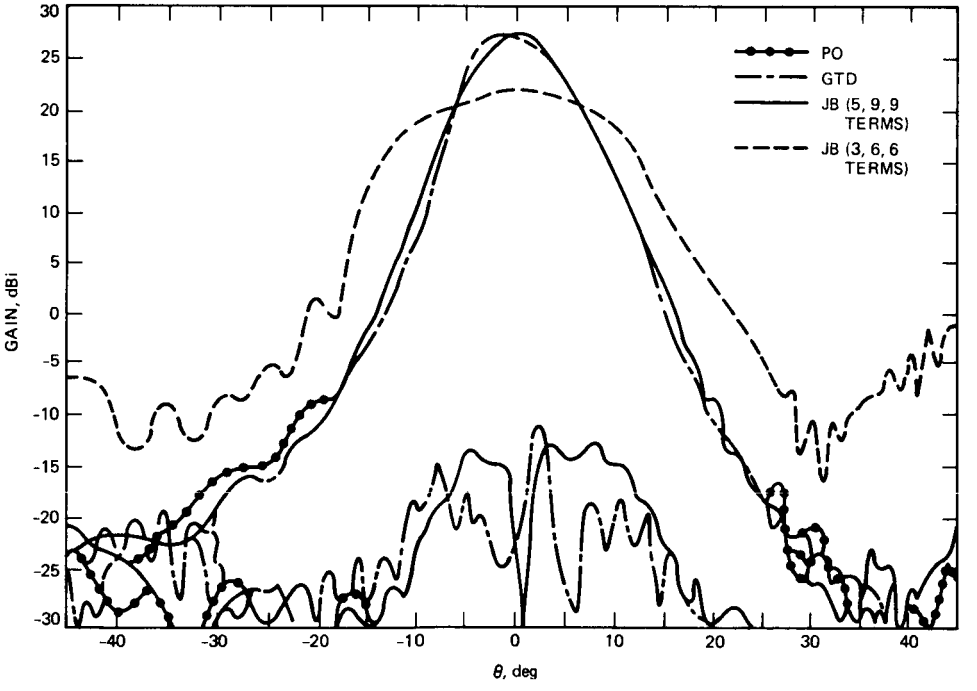

Fig. 13. Far-field, one 2.4-m ellipse diffraction patterns (RCP, 2.3-GHz, offset plane)

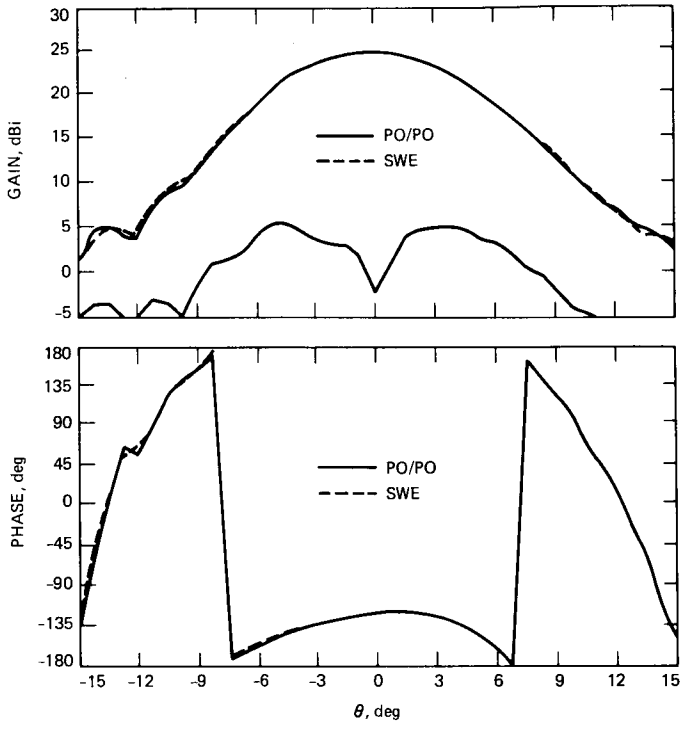

Fig. 14. PO and SWE near-field scattering from a single 2.4-m paraboloid at 2.3 GHz: (a) amplitude; (b) phase

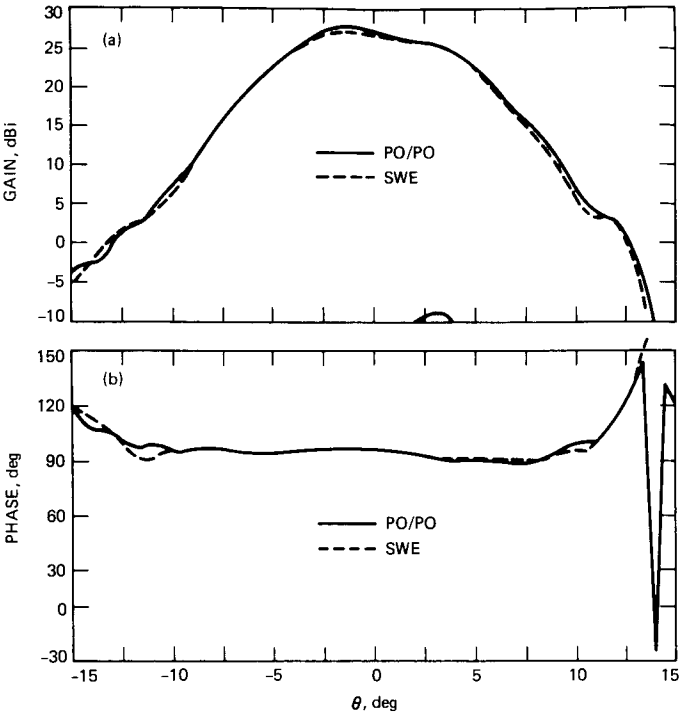

Fig. 15. PO and SWE far-field scattering from two 2.4-m paraboloids at 2.3 GHz: (a) amplitude; (b) phase

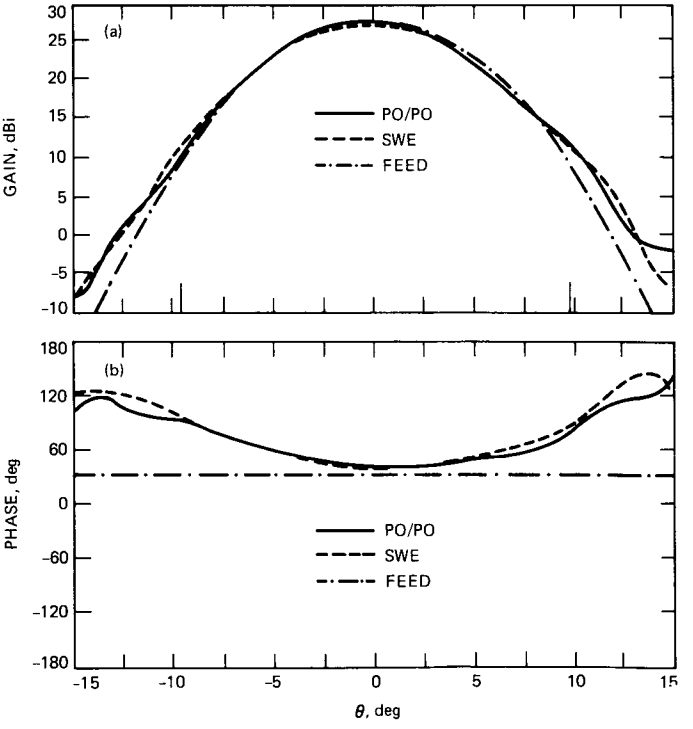

Fig. 16. PO and SWE near-field scattering from two 2.4-m paraboloids at 2.3 GHz (comparison with feed pattern): (a) amplitude; (b) phase

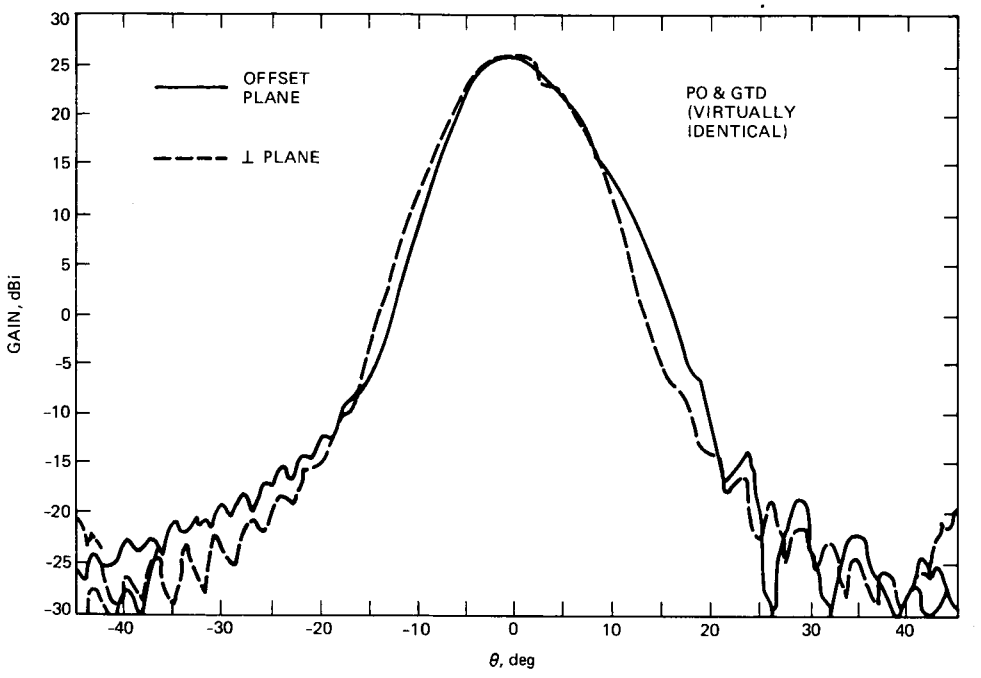

Fig. 17. Near-field, one 2.4-m ellipse diffraction patterns (RCP, 8.4 GHz, offset and plane cuts)

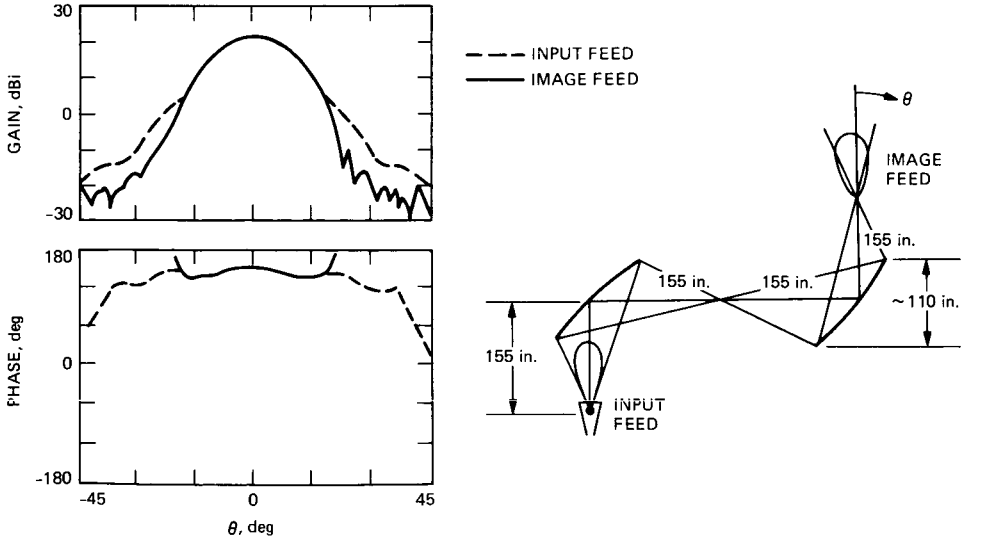

Fig. 18. GTD scattering for two 2.4-m ellipses, RCP at 8.4 GHz